E12-11-007 Jeopardy Update to PAC50

Asymmetries in Semi-Inclusive Deep-Inelastic $(e, e'\pi^{\pm})$ Reactions on a Longitudinally Polarized ^{3}He Target at 8.8 and 11 GeV

Spokespersons:

Jin Huang

Brookhaven National Lab, Upton, NY

Jian-ping Chen* (Contact), Yi Qiang

Thomas Jefferson National Accelerator Facility, Newport News, VA

Chao Peng

Argonne National Laboratory, Lemont, IL

Wenbiao Yan

University of Science and Technology of China, Hefei, China

(The SIDIS-Longitudinal-He3 Collaboration †)

*jpchen@jlab.org

†see the full collaboration list at https://solid.jlab.org/collaboration/sidis-long-he3.html

1 Introduction

Experiment E12-11-007 [1], a semi-inclusive deep inelastic scattering (SIDIS) measurement by employing a longitudinally polarized ^{3}He target at incident electron beam energies of 8.8 and 11 GeV, was approved by PAC39 with A rating. This experiment will measure one target single-spin asymmetry (SSA) and two beam-target double spin asymmetries (DSAs) of π^+/π^- particles produced in SIDIS processes using the proposed Solenoidal Large Intensity Device (SoLID) apparatus [2, 3]. Since the approval of E12-11-007, there has been one run group experiment approved, and it is E12-11-007A on g_2^n and d_2^n measurements. The ultimate measurement results to be obtained from both experiments will add valuable and essential "neutron" information to the world data (together with the upcoming results from the SoLID SIDIS experiment E12-10-006 on a transversely polarized ^{3}He target and its associated run group experiments). We first describe the latest design of the SoLID apparatus and the SoLID status. Then we present an update on E12-11-007 experiment, followed by a brief update on the associated run group experiment.

2 Progress on the SoLID Apparatus

Since the approval in 2010 of five SoLID experiments with high rating by the JLab PAC, the collaboration has developed a Pre-CDR [3], which gives details on the SoLID apparatus as well as a cost estimate. In 2015, SoLID together with the approved experiments received a strong endorsement from the Nuclear Physics Long Range Plan. In September of 2019, the Pre-CDR successfully passed the second of two JLab Director's Reviews. The latter review covered a detailed cost estimate and detailed analysis, which concluded that all critical items were low risk. The Pre-CDR was the basis of the SoLID MIE submitted to the DOE in February of 2020. In 2020, the DOE funded a Pre-R&D plan, which has demonstrated that there are no show-stoppers in the design of SoLID. In March of 2021, the DOE performed the Science Review of SoLID. We give a brief overview of the features of the SoLID apparatus and Pre-R&D progress below.

In the Pre-CDR, we have demonstrated that the apparatus can achieve the following goals:

1. High luminosity (10^{37} cm^{-2}s^{-1} for SIDIS and J/ψ, 10^{39} cm^{-2}s^{-1} for PVDIS with baffles);
2. Large acceptance: 2π in azimuthal angle ϕ; in polar angle θ: $8^\circ - 24^\circ$ for SIDIS and J/ψ, $22^\circ - 35^\circ$ for PVDIS; momentum range: $1 - 7$ GeV/c;
3. High rates (trigger rate limit 100 KHz for SIDIS and J/ψ, 600 KHz of the 30 sectors for PVDIS);
4. High background tolerance ($\sim$1 GHz, dominated by low energy photons/electrons);
5. High radiation environment tolerance (10^{2-3} krad);
6. Moderate resolutions ($1 - 2\%$ in momentum, $1 - 2$ mrad in θ, 6 mrad in ϕ);
7. Good electron PID, moderate pion PID (SIDIS), and demanding Kaon PID (SIDIS-Kaon, enhanced configuration);
8. High precision with low systematic effects.

• The SoLID apparatus in its SIDIS configuration with a ^{3}He target is shown in Fig. 1 Since the SoLID experiments were approved, the CLEOII magnet was chosen. It was moved to JLAB in 2016. JLAB is currently performing refurbishment of the magnet and preparing for a cold test to

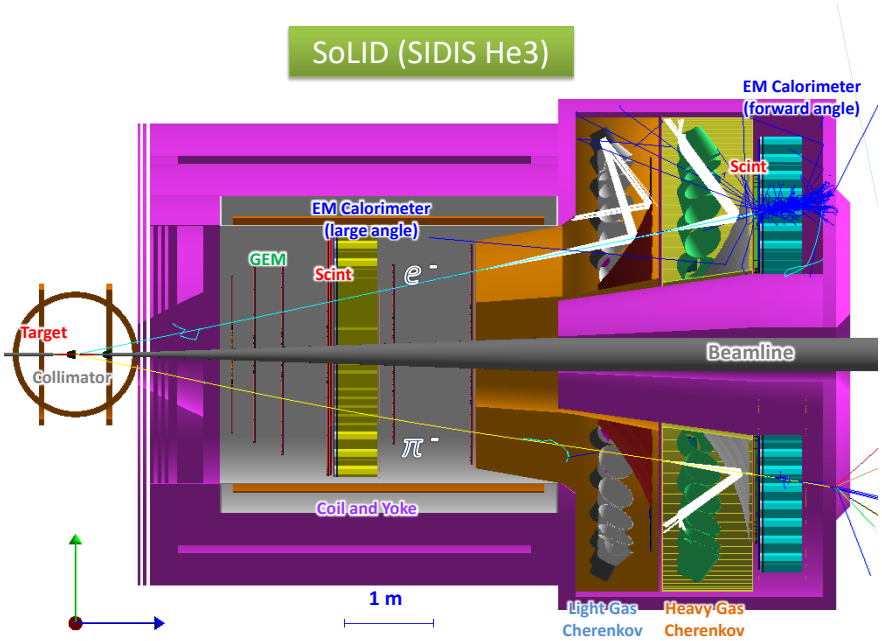

Figure 1: SoLID SIDIS Setup with ^{3}He target.

establish the magnet's operational condition. The cold test is scheduled to be completed by the end of 2022.

• Significant progress has been made in all subsystems, and components have been tested and shown to meet specifications. UVa group has built large GEM chambers with sizes what SoLID needs. They also successfully built and operated GEM detectors for the PRad experiment and SBS experiment. During recent execution of the Pre-R&D plan, we have tested new VMM3 GEM readout chips, which we plan to use instead of the obsolete APV25 chips listed in the original proposals. We have demonstrated that with the VMM3 chips operated in a mode with a 25 ns shaping time, the readout can handle the high rates required for SoLID.

• A prototype Čerenkov was tested with a beam at JLab Hall C in 2020, both at low rates and also at high rates equal to those expected in the SoLID spectrometer. In both the low- and high-rate configurations, clean signals could be identified, the detector and readout system performed very well.

• The ECal prototype modules were successfully tested at the Fermilab Test Beam Facility in January of 2021. Data showed that the energy resolution of the 3-module setup reached the SoLID requirement of $\delta E/E = \sqrt{10\%}/\sqrt{E}$ and the position resolution exceeded the required 1 cm specification.

• The SoLID DAQ system is based on the JLab 12 GeV FADC base pipelined electronics, which now has been successfully used in Halls B and D. Special features of the JLab FADC required for SoLID, which were built into the JLab design but never used in previous applications, have now been successfully tested for all systems as part of the SoLID Pre-R&D plan.

• Currently, a beam test of a full set of the SoLID detector prototypes – GEM, LGC, ECal, DAQ and associated electronics – is in preparation. The goal of the test is to fully characterize the functionality of the detector system under a high-rate, high-radiation environment that is similar

to SoLID operation.

• The SoLID simulation software, based on GEMC/GEANT4, is a single package that is used to model all approved experiments and run-group experiments. It is being used to optimize the design and evaluate the impact of the results from the past and ongoing tests. A Kalman Filter based track finding and fitting algorithm has been developed and tested with fully digitized GEM simulation data. Tracking resolutions with a good tracking efficiency have been obtained with the background taken into account. We are actively working on assembling simulation, reconstruction, and analysis into one software framework.

3 Update on Experiment E12-11-007

3.1 One SSA and two DSAs to be measured in SoLID

SIDIS is a process that describes a lepton scattered off a nucleon target, in which the scattered lepton and a leading final-state hadron are detected, providing a powerful tool to probe the constituents' longitudinal and transverse momenta and spin structure of the nucleon. In such a process, high-precision scattering experiments can extract the transverse-momentum-dependent parton distribution function (TMD PDFs, or TMDs), which reveal the 3-D tomography of the nucleon in momentum space. Most TMDs exist due to couplings of the quark transverse momentum with the spins of the nucleon and quark. Thereby, the TMDs link the intrinsic transverse motion of partons to their spins and the spin of the parent nucleon. In this case, one can study the spin-orbit correlations in QCD.

At leading twist, there are eight TMDs, grouped with their characteristic quark and target-nucleon spin combinations. If we integrate these functions over the quark transverse momentum inside the nucleon, TMDs that survive this integration are the unpolarized PDF f_1, the longitudinally polarized PDF g_{1L} (a.k.a. Helicity), and the transversely polarized PDF h_1 (a.k.a. Transversity) [4]. Fig. 2 tabulates all the eight TMD functions according to the quark and nucleon polarizations, where U stands for unpolarized, L and T for longitudinal and transverse polarization, respectively. All of them are functions of the longitudinal momentum fraction x (Bjorken x), and the quark transverse momentum $\mathbf{k}_\perp$. There are five additional leading-twist TMDs [5, 6] other than the f_1, g_{1L} and h_1. These five TMDs provide novel information on the spin-orbit correlations.

For example, the Worm-gear functions, g_{1T} and $h_{1L}^\perp$ seen in Fig. 2, describe the probability of finding a longitudinally polarized quark inside a transversely polarized nucleon, as well as finding a transversely polarized quark inside a longitudinally polarized nucleon, respectively. They provide important information to understand the correlations among the quark OAM, the quark spin and the nucleon spin. More specifically, both of the Worm-gear functions require an interference between wave function components that differ by one unit of quark OAM, as explicitly shown in several models in Refs. [7–9].

Experimental information on the Worm-gear TMD functions $h_{1L}^\perp$, g_{1T} and the Helicity g_{1L} can be obtained through measurements of some SIDIS azimuthal asymmetries of charged hadrons on a longitudinally polarized ^{3}He target. Fig. 3 demonstrates the SIDIS process given in terms of azimuthal angles defined to the lepton scattering plane. ϕ_h is an angle between the lepton scattering plane and the hadron production plane, whereas ϕ_S is an angle between the lepton scattering plane and the polarization vector of the target's spin. The Worm-gear $h_{1L}^\perp$ can be accessed through

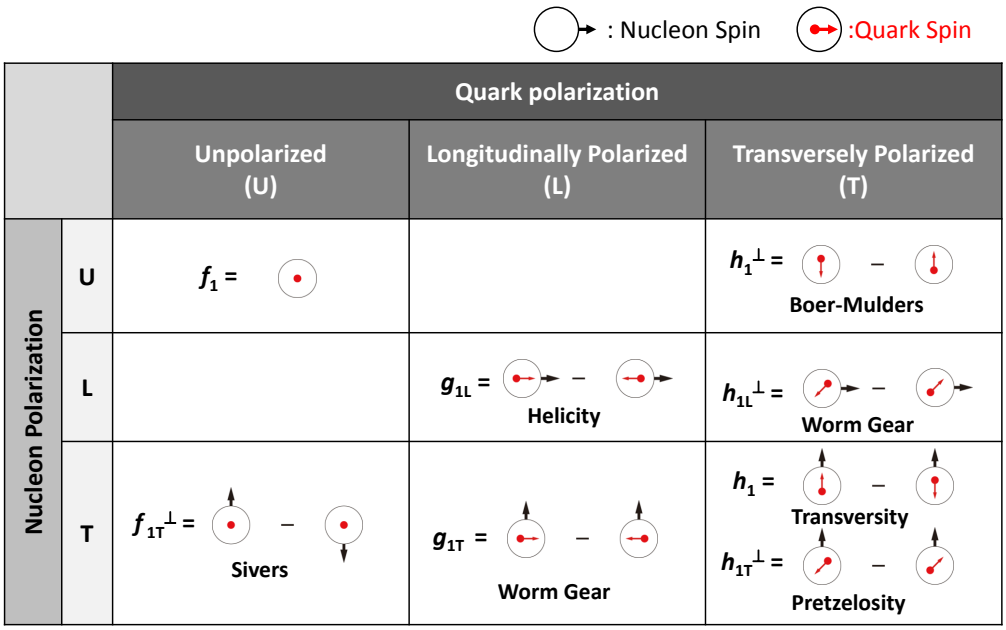

Figure 2: Illustration of spin correlations of eight leading twist TMDs arranged according to the quark (U, L, T) and nucleon (U, L, T) polarizations. The red arrows indicate the spin direction of quarks; black arrows indicate the spin direction of the parent (target) nucleon.

measurements of the SSA A_{UL} with the $\sin(2\phi_h)$ angular modulation ($A_{UL}^{sin(2\phi_h)}$); the Worm-gear g_{1T} can be accessed through measurements of the DSA A_{LT} with the $\cos(\phi_h - \phi_S)$ modulation ($A_{LT}^{\cos(\phi_h-\phi_S)}$); and the Helicity g_{1L} can be accessed through measurements of the DSA A_{LL} with the modulation equal to 1.

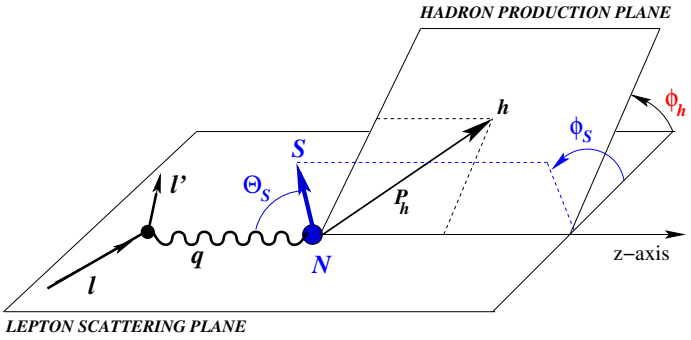

Figure 3: Kinematics of the SIDIS process sketched in the one-photon exchange approximation, showing how the azimuthal angles are defined in the target rest frame. This figure is from Ref. [10].

The aforementioned three asymmetries stand in the SIDIS differential cross section among the other fifteen terms [10]. Let us just show only these three terms, at leading order in $1/Q$, in the SIDIS cross-section formula that are relevant to our proposal:

$$\frac{d\sigma_{\rm SIDIS}}{dx\,dy\,dz\,dP_{h\perp}^2\,d\phi_h\,d\phi_S} = \frac{\alpha^2}{xyQ^2}\left(1-y+\frac{1}{2}y^2\right)F_{UU}(x,y,P_{h\perp}^2)\times$$
$$\left\{1+...+S_L\sin(2\phi_h)p_1A_{UL}^{\sin(2\phi_h)}+\lambda_e\,S_L\,p_2A_{LL}+...+\lambda_eS_T\cos(\phi_h-\phi_S)p_2A_{LT}^{\cos(\phi_h-\phi_S)}+...\right\}, \quad (1)$$

where S_L and S_T are the longitudinal and transverse components of the target-spin direction, λ_e is the helicity of the lepton beam. The kinematic invariants are

$$x=\frac{Q^2}{2P\cdot q}, \qquad y=\frac{P\cdot q}{P\cdot l}, \qquad z_h=\frac{P\cdot P_h}{P\cdot q}, \qquad Q^2=-q^2. \quad (2)$$

For the definitions of all prefactors p_i, see Eq. (2.3) in [10]. The three asymmetries shown in Eq. (1) are defined via the SIDIS structure functions given by

$$A_{UL}^{\sin(2\phi_h)} \equiv \varepsilon\,\frac{F_{UL}^{\sin(2\phi_h)}}{F_{UU}} \propto h_{1L}^{\perp}\otimes H_1^{\perp}, \quad (3)$$

$$A_{LT}^{\cos(\phi_h-\phi_S)} \equiv \sqrt{1-\varepsilon^2}\,\frac{F_{LT}^{\cos(\phi_h-\phi_S)}}{F_{UU}} \propto g_{1T}\otimes D_1, \quad (4)$$

$$A_{LL} \equiv \sqrt{1-\varepsilon^2}\,\frac{F_{LL}}{F_{UU}} \propto g_{1L}\otimes D_1, \quad (5)$$

(see Sec. 1.1 and Sec. 1.2 of [1] for more details), where $H_1^{\perp}$ is the Collins fragmentation function [11], D_1 is the unpolarized fragmentation function. ε is the ratio of the longitudinal and transverse photon fluxes, which is expressed via a specific combination of the prefactors p_i [12].

3.2 Some details on E12-11-007

Experiment E12-11-007 has been approved for 35 days of total beam time with 15 μA, 11/8.8 GeV electron beams on a 40-cm long, 10 amgs longitudinally polarized ^{3}He target to match about a similar level of statistics of the experiment E12-10-006 [13]. In particular, with the 35 PAC days of longitudinally polarized data, the statistical precision of $A_{UL}^{sin(2\phi_h)}$ and A_{LL} will reach 50% of statistics of the SSA measurements in E12-10-006. In addition, $A_{LT}^{cos(\phi_h-\phi_S)}$ can be cleanly disentangled from A_{LL} by combining both the transverse and longitudinal target-spin data. When combined with E12-10-006, this experiment will not require any beam time for data calibration, including reference cell runs and detector calibrations. The projected data are binned into 4-D $(x, P_{h\perp}, z, Q^2)$ bins. The table shown in Fig. 4 summarizes the budget for systematic uncertainties. The SoLID apparatus will provide improvements on systematic uncertainty determination, which comes from the target's fast spin flip ($\leq$ 20 mins for the ^{3}He target). Also, there will be reduction of systematic uncertainties in extraction of different angular modulation terms, coming from the full (2π) coverage in the spin azimuthal angle, as well as coming from the large coverage in the hadron azimuthal angle. Besides, one can obtain additional reduction of the systematic uncertainties, if the asymmetries measured for both π^+ and π^- are combined for a u and d quark flavor separation.

For having more details on how the systematic uncertainty from each of the shown sources in Fig. 4 has been estimated for the three asymmetries under consideration, we refer to Sec. 4 of

the original proposal [1]. But here one should note that the statistical uncertainty for a typical bin is determined to be larger than the systematic uncertainties. Namely, the absolute statistical uncertainty for $A_{UL}^{sin(2\phi_h)}$ is 5×10^{-3}, for $A_{LT}^{cos(\phi_h-\phi_S)}$ is 4×10^{-3}, and for A_{LL} is 4×10^{-3} (with 1000-1400 4-D bins for A_{LL}, A_{UL} or A_{LT}).

Source (Type): ^{3}He (E12-11-007)	$A_{UL}^{sin(2\phi_h)}$ π^+ / π^-	$A_{LT}^{cos(\phi_h-\phi_S)}$ π^+ / π^-	A_{LL} π^+ / π^-
Raw asymmetry (Abs.)	1×10^{-3}	negligible	negligible
Random coincidence (Rel.)	1%	1%	1%
Polarimetry (Rel.)	3%	4%	4%
Nuclear effects (Rel.)	4%	4%	4%
Diffractive meson (Rel.)	3%	3%	3%
Radiative corrections (Rel.)	2%	3%	3%
Total (Abs.) / Total (Rel.)	1×10^{-3} / 6.2%	negligible / 7.1%	negligible / 7.1%

Figure 4: The budget for the absolute and relative systematic uncertainties of the one π^+/π^- SSA and two π^+/π^- DSAs under consideration.

For a typical z and Q^2 bin ($0.40 < z < 0.45$, 2 GeV^2 $< Q^2 <$ 3 GeV^2, some selected data projections are shown in Fig. 5 (for $A_{UL}^{sin(2\phi_h)}$ and A_{LL}) as well as in Fig. 6 (for $A_{LT}^{cos(\phi_h-\phi_S)}$). The center of each red point corresponds to the kinematic center of each x and $P_{h\perp}$ bin, and the error bar corresponds to the statistical uncertainty of the asymmetry for each $(x, P_{h\perp}, z, Q^2)$ bin. The scale of the asymmetries and uncertainties is shown on the right-side axis. For the complete projections, we refer to Appendix B of the original proposal [1].

In the left panel of Fig. 5, the blue curve is a predicted asymmetry with light-cone constituent quark models, evaluated at $Q^2 = 2.5$ GeV^2 and $z = 0.5$ by Barbara Pasquini, *et. al.* [8, 9]; the black curves (solid and dash represent two approaches of parametrizations) are predicted asymmetries with a light-cone quark-diquark model with the Melosh-Wigner rotation effect [14, 15] taken into account, calculated by Bo-Qiang Ma, *et. al.* [16]; the magenta dash-dotted curve is a prediction based on the Wandzura-Wilczek (WW)-type relations by Alexei Prokudin, *et. al.* [10, 17]. All theory predictions are integrated over $P_{h\perp}$. In the right panel of Fig. 5, the blue lines show a $P_{h\perp}$-integrated A_{LL} prediction at $Q^2 = 2$ GeV^2 and $z = 0.425$, based on the next-to-leading order (NLO) parametrization of unpolarized parton distribution function (PDF) [18], polarized PDF [19] and unpolarized fragmentation function (FF) [20]. In both panels of Fig. 6, the explanation of theoretical predictions is the same as in the left panel of Fig. 5. Also shown black data points are the statistical uncertainties of the data from the JLab 6 GeV experiment E06-010 [21].

3.3 First global extraction of the Worm-gear TMD to be updated with SoLID projection data

In Ref. [22], the first global extraction of g_{1T} has been carried out, using all experimental measurements available, namely $A_{LT}^{cos(\phi_h-\phi_S)}$ data from COMPASS [23], HERMES [24], and JLab [21]. The so-called weighted χ^2 method was applied to allow the JLab data, which has four data points, to also contribute on the same footing as the HERMES and COMPASS data sets. One of

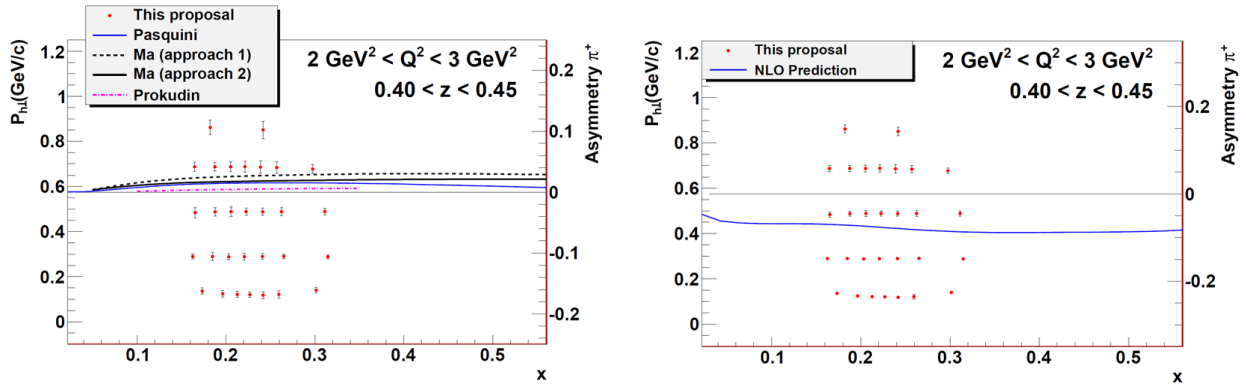

Figure 5: SoLID SIDIS projections in a typical z and Q^2 bin ($0.40 < z < 0.45$, 2 GeV^2 $< Q^2 <$ 3 GeV^2) for the π^+ SSA $A_{UL}^{sin(2\phi_h)}$ (left panel) and π^+ DSA A_{LL} (right panel) measurements as a function of x, with different ranges of the hadron $P_{h\perp}$ labeled.

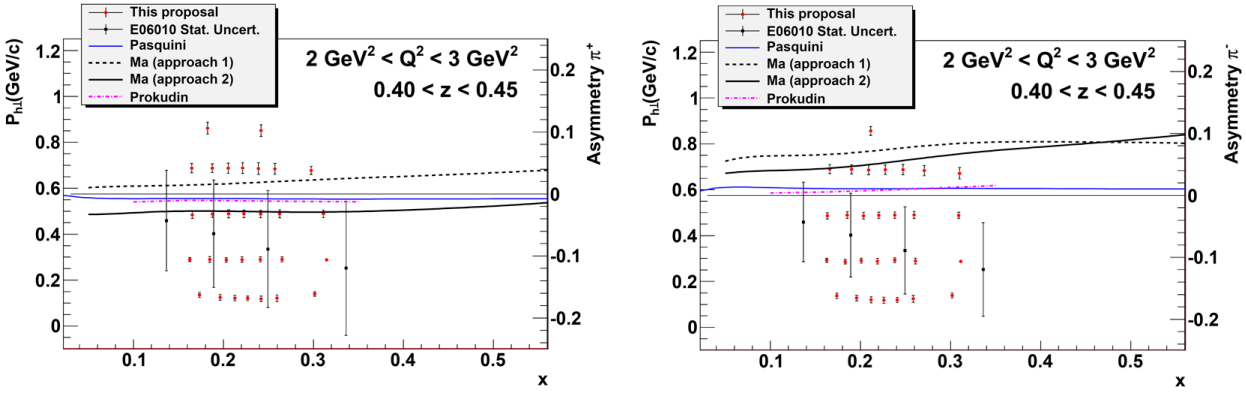

Figure 6: SoLID SIDIS projections in a typical z and Q^2 bin ($0.40 < z < 0.45$, 2 GeV^2 $< Q^2 <$ 3 GeV^2) for the π^+/π^- DSA $A_{LT}^{cos(\phi_h-\phi_S)}$ measurements as a function of x, with different ranges of the hadron $P_{h\perp}$ labeled.

the main conclusions of [22] is that g_{1T} is positive for the u quark and negative for the d quark. with g_{1T} of the u quark being somewhat larger in magnitude than that of the d quark. Another important conclusion is that a fitted value (see the blue circle point in Fig. 7) for the Worm-gear shift, given by

$$\left[\langle k_x\rangle_{TL}\right](Q^2) = M_N \frac{\int_0^1 dx\left[g_{1T}^u(x,Q^2) - g_{1T}^d(x,Q^2)\right]}{\int_0^1 dx\left[f_1^u(x,Q^2) - f_1^d(x,Q^2)\right]}, \tag{6}$$

is compatible with a result obtained from Lattice QCD (LQCD). There is a discrepancy between the LQCD calculation (green triangle point) and the calculations using the WW-type approximation (red square points). The fitted value is in good agreement with the calculations using the WW-type approximation and in agreement with the LQCD calculation within the large uncertainty. The projected precise SoLID data on $A_{LT}^{cos(\phi_h-\phi_S)}$ (Fig. 6) should significantly improve the precision on the global fit of the shift. The SoLID collaboration will closely work with our theory colleagues (who published Ref. [22] recently) to achieve the anticipated update of Fig. 7 in the near future.

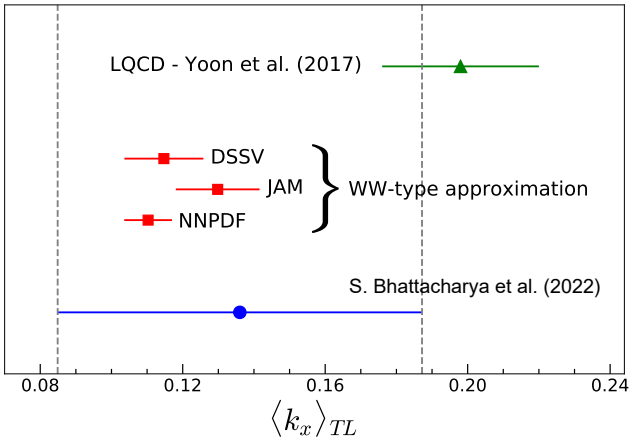

Figure 7: Comparison of the Worm-gear shift $\langle k_x \rangle_{TL}$ calculated using the main fit in [22], described by the blue circle point, with the shifts calculated within the WW-type approximation in [22], described by the red square points, as well as with the shift calculated in LQCD (green triangle points) (see Fig. 13 of [25]).

4 Run group experiment g2n and d2n: E12-11-007A

(**Spokespersons:** Chao Peng, Ye Tian (Contact))

The transverse polarized structure function $g_2(x, Q^2)$ probes transversely and also longitudinally polarized parton distributions inside the nucleon. It carries information on quark–gluon interactions inside the nucleon. By neglecting quark masses, $g_2(x, Q^2)$ can be decoded by a leading twist–2 term and a higher twist term as follows:

$$g_2(x, Q^2) = g_2^{WW}(x, Q^2) + \bar{g_2}(x, Q^2), \tag{7}$$

where twist–2 term g_2^{WW} has been derived by Wandzura and Wilczek [26], and it only depends on well–measured g_1 [27, 28].

Matrix Element d_2 is the x^2 moment of $\bar{g_2}(x, Q^2)$. This quantity measures deviations of $g_2(x, Q^2)$ from the twist–2 term g_2^{WW}. At large Q^2, where the operator product expansion (OPE) [29] becomes valid, one can access the twist–3 effects of quark–gluon correlations via the third moment of a linear combination of $g_1(x, Q^2)$ and $g_2(x, Q^2)$, presented as

$$d_2(Q^2) = 3\int_0^1 x^2[g_2(x, Q^2) - g_2^{WW}(x, Q^2)]dx = \int_0^1 x^2[2g_1(x, Q^2) + 3g_2(x, Q^2)]dx. \tag{8}$$

Due to the x^2–weighting, $d_2(Q^2)$ is particularly sensitive to the large–x behavior of $\bar{g_2}$ and provides us a clean way to access twist–3 contribution.

The direct extraction of g_2 requires the cross-section differences measured in both the parallel ($\Delta\sigma_\parallel$) and perpendicular ($\Delta\sigma_\perp$) configurations, in which the target is polarized longitudinally and transversely with respect to the beam direction, respectively. This proposed run-group experiment will measure the parallel cross-section difference inclusively with single-electron triggers, taking data simultaneously with the experiment E12-10-006 [13]. Such data will then be combined with the perpendicular cross-section difference data also taken from E12-10-006, which has proposed the same beam energies and detector configurations with a transversely polarized ^{3}He target, to extract neutron structure functions.

Assuming $\cos(\phi_{rela}) = 1$, the extraction of g_1 and g_2 can be written as:

$$
\begin{aligned}
g_1 &= \frac{MQ^2}{4\alpha^2}\frac{\nu E}{(E-\nu)(2E-\nu)}\left[\Delta\sigma_{\parallel} + \tan\frac{\theta}{2}\Delta\sigma_{\perp}\right], \\
g_2 &= \frac{MQ^2}{4\alpha^2}\frac{\nu^2}{2(E-\nu)(2E-\nu)}\left[-\Delta\sigma_{\parallel} + \frac{E+(E-\nu)\cos\theta}{(E-\nu)\sin\theta}\Delta\sigma_{\perp}\right].
\end{aligned}
\tag{9}
$$

The spin-dependent structure function g_2 heavily relies on the perpendicular cross-section difference $\Delta\sigma_{\perp}$ due to the large kinematic factor within the proposed kinematic coverage, while the g_1 is mostly dependent on $\Delta\sigma_{\parallel}$. Therefore, the statistical and systematic uncertainties of g_2 are dominated by those of $\Delta\sigma_{\perp}$.

A precision measurement of the neutron spin structure function $g_2(x, Q^2)$, running in parallel with this experiment and experiment E12-10-006, has been approved as a run group proposal [30] by PAC48. High-statistics data will be collected within a large kinematic coverage of Bjorken scaling $x > 0.1$ and four-momentum transfer $1.5 < Q^2 < 10$ GeV^2 from inclusive scatterings of longitudinally polarized electrons off longitudinally and transversely polarized ^{3}He targets, at incident beam energies of 11 GeV and 8.8 GeV. In addition to mapping out the x and Q^2 evolution of g_2, the moment $d_2(Q^2)$, which is connected to the quark-gluon correlations within the nucleon, will be extracted with $1.5 < Q^2 < 6.5$ GeV^2. $d_2(Q^2)$ is one of the cleanest observables that can be used to test the theoretical calculations from lattice QCD and various nucleon structure models.

5 Summary

In the SoLID SIDIS experiment E12-11-007, the data on $A_{UL}^{sin(2\phi_h)}$ and $A_{LT}^{cos(\phi_h-\phi_S)}$ asymmetries will provide long-awaited important information to understand the correlations among the quark OAM, the quark spin and nucleon spin. High-precision data will expand our current knowledge of the nucleon spin structure in terms of the orbital motions of underlying partons described by the QCD dynamics. In addition, the A_{LL} asymmetry data will in turn improve our knowledge on the precision of global analysis for nucleon helicity distribution extractions, especially for the d quark. Furthermore, we will be working with the authors of Ref. [22] to include this proposal's projection data (SoLID $A_{LT}^{cos(\phi_h-\phi_S)}$) into their very recent global QCD analysis for extraction of the Worm-gear g_{1T} TMD function. Besides, with the pertinent run group experiment on g_2 and d_2, we will be able to study polarized parton distributions inside the nucleon to reach deeper understanding of quark–gluon interactions, taking also into account that the observable d_2 is calculable in LQCD.

References

[1] J.-P. Chen (contact), J. Huang, Y. Qiang, and W. B. Yan, Jefferson Lab Experiment E12-11-007, URL https://solid.jlab.org/experiments.html.

[2] J. P. Chen, H. Gao, T. K. Hemmick, Z. E. Meziani, and P. A. Souder (SoLID) (2014), 1409.7741.

[3] The SoLID Collaboration, SoLID (Solenoidal Large Intensity Device) Updated Preliminary Conceptual Design Report, Jefferson Lab Hall A SoLID Experiment, URL https://solid.jlab.org/.

[4] H. Gao et al., Eur. Phys. J. Plus **126**, 2 (2011), 1009.3803.

[5] P. J. Mulders and R. D. Tangerman, Nucl. Phys. B **461**, 197 (1996), [Erratum: Nucl.Phys.B 484, 538–540 (1997)], hep-ph/9510301.

[6] D. Boer and P. J. Mulders, Phys. Rev. D **57**, 5780 (1998), hep-ph/9711485.

[7] A. Bacchetta, F. Conti, and M. Radici, Phys. Rev. D **78**, 074010 (2008), 0807.0323.

[8] B. Pasquini, S. Cazzaniga, and S. Boffi, Phys. Rev. D **78**, 034025 (2008), 0806.2298.

[9] S. Boffi, A. V. Efremov, B. Pasquini, and P. Schweitzer, Phys. Rev. D **79**, 094012 (2009), 0903.1271.

[10] S. Bastami et al., JHEP **06**, 007 (2019), 1807.10606.

[11] J. C. Collins, Nucl. Phys. B **396**, 161 (1993), hep-ph/9208213.

[12] A. Bacchetta, M. Diehl, K. Goeke, A. Metz, P. J. Mulders, and M. Schlegel, JHEP **02**, 093 (2007), hep-ph/0611265.

[13] J.-P. Chen, H. Gao (contact), X. Jiang, J. C. Peng, and A. Qian, Jefferson Lab Experiment E12-10-006, URL https://solid.jlab.org/experiments.html.

[14] B.-Q. Ma, J. Phys. G **17**, L53 (1991), 0711.2335.

[15] B.-Q. Ma, Z. Phys. C **58**, 479 (1993), hep-ph/9306241.

[16] J. She, J. Zhu, and B.-Q. Ma, Phys. Rev. D **79**, 054008 (2009), 0902.3718.

[17] A. Kotzinian, B. Parsamyan, and A. Prokudin, Phys. Rev. D **73**, 114017 (2006), hep-ph/0603194.

[18] A. D. Martin, W. J. Stirling, R. S. Thorne, and G. Watt, Eur. Phys. J. C **63**, 189 (2009), 0901.0002.

[19] J. Blumlein and H. Bottcher, Nucl. Phys. B **636**, 225 (2002), hep-ph/0203155.

[20] D. de Florian, R. Sassot, and M. Stratmann, Phys. Rev. D **75**, 114010 (2007), hep-ph/0703242.

[21] J. Huang et al. (Jefferson Lab Hall A), Phys. Rev. Lett. **108**, 052001 (2012), 1108.0489.

[22] S. Bhattacharya, Z.-B. Kang, A. Metz, G. Penn, and D. Pitonyak, Phys. Rev. D **105**, 034007 (2022), 2110.10253.

[23] C. Adolph et al. (COMPASS), Phys. Lett. B **770**, 138 (2017), 1609.07374.

[24] A. Airapetian et al. (HERMES), JHEP **12**, 010 (2020), 2007.07755.

[25] B. Yoon, M. Engelhardt, R. Gupta, T. Bhattacharya, J. R. Green, B. U. Musch, J. W. Negele, A. V. Pochinsky, A. Schäfer, and S. N. Syritsyn, Phys. Rev. D **96**, 094508 (2017), 1706.03406.

[26] S. Wandzura et al., Physics Letters B **72**, 195 (1977).

[27] B. Adeva et al. (Spin Muon Collaboration), Phys. Rev. D **58**, 112001 (1998).

[28] K. Abe et al. (E143 Collaboration), Phys. Rev. D **58**, 112003 (1998).

[29] K. G. Wilson et al., Phys. Rev. **179**, 1499 (1969), URL https://link.aps.org/doi/10.1103/PhysRev.179.1499.

[30] Y. Tian et al., *A run-group proposal submitted to PAC 48*, https://www.jlab.org/exp_prog/proposals/20/E12-11-007A_E12-10-006E_Proposal.pdf.